

PDF hosted at the Radboud Repository of the Radboud University Nijmegen

The following full text is an author's version which may differ from the publisher's version.

For additional information about this publication click this link.

<http://hdl.handle.net/2066/99115>

Please be advised that this information was generated on 2019-04-20 and may be subject to change.

Accumulation of Stark-decelerated NH molecules in a magnetic trap

Jens Riedel^{1,2}, Steven Hoekstra^{1,3}, Wolfgang Jäger⁴, Joop J. Gilijamse¹, Sebastiaan Y.T. van de Meerakker¹, and Gerard Meijer¹

¹ Fritz-Haber-Institut der Max-Planck-Gesellschaft, Faradayweg 4-6, D-14195 Berlin, Germany

² Present address: Bundesanstalt für Materialforschung und -prüfung, Richard-Willstätter-Str. 11, D-12489 Berlin, Germany

³ Present address: Kernfysisch Versneller Instituut, Rijksuniversiteit Groningen, Zernikelaan 25, 9747 AA Groningen, The Netherlands

⁴ Department of Chemistry, University of Alberta, Edmonton, Alberta, Canada T6G 2G2

Received: date / Revised version: date

Abstract. Here we report on the accumulation of ground-state NH molecules in a static magnetic trap. A pulsed supersonic beam of NH ($a^1\Delta$) radicals is produced and brought to a near standstill at the center of a quadrupole magnetic trap using a Stark decelerator. There, optical pumping of the metastable NH radicals to the $X^3\Sigma^-$ ground state is performed by driving the spin-forbidden $A^3\Pi\leftarrow a^1\Delta$ transition, followed by spontaneous $A \rightarrow X$ emission. The resulting population in the various rotational levels of the ground state is monitored via laser induced fluorescence detection. A substantial fraction of the ground-state NH molecules stays confined in the several milliKelvin deep magnetic trap. The loading scheme allows one to increase the phase-space density of trapped molecules by accumulating packets from consecutive deceleration cycles in the trap. In the present experiment, accumulation of six packets is demonstrated to result in an overall increase of only slightly over a factor of two, limited by the trap-loss and reloading rates.

1 Introduction

Cold and ultra-cold atoms have had a major impact on modern physics and the ensuing studies have revolutionized our view of the quantum world. An analogous generation of studies on cold and ultra-cold neutral molecules promises to have similar, perhaps even farther reaching, consequences. The added degrees of freedom in molecular systems, such as rotation, vibration and electric and magnetic moments, provide additional handles by which to manipulate them. For these reasons, research on cold and ultra-cold molecules has rapidly become a mature research field [1].

Cold and ultra-cold molecules are anticipated to have widespread applications, and the field is characterized by the enormous variety of experimental methods that have been developed to produce samples of these. The atomic physicists in this field have perfected the methods to assemble ultra-cold molecules from ultra-cold atoms using photoassociation or association through magnetically tuned Feshbach resonances. These methods are limited mainly to alkali atoms, but can produce dense samples of molecules in the ultra-cold regime [2]. The molecular physicists have developed methods to bring pre-existing molecules to low temperatures by, for instance, thermalizing them with a cryogenic buffergas [3] or by manipulating their motion with external fields [4]. While applicable to a wider variety of molecular systems, these techniques only reach into

the cold (1 mK - 1 K) regime with considerable lower number densities. Nevertheless, these methods can be used to load neutral molecules into magnetic or electrostatic traps in which a further phase space density increase might be obtained via cooling through, for example, evaporative or laser cooling [5].

An alternative approach to increase the phase space density of trapped ground-state molecules is to add new molecules to the trap, without losing or heating the ones that are already trapped. Here, we experimentally demonstrate the accumulation of ground-state NH radicals in a magnetic trap, following a detailed proposal and ending a ten year quest [6]. The essence of the proposal is that NH ($a^1\Delta$) radicals, brought to a standstill using electric fields, can be transferred to the $X^3\Sigma^-$ ground state via optical pumping on the spin-forbidden $A^3\Pi\leftarrow a^1\Delta$ transition followed by spontaneous emission to the ground state. This laser induced spontaneous emission process provides a unidirectional path from the metastable state to the ground state of NH. In their ground state, the NH radicals are hardly influenced by electric fields, but can be trapped using magnetic fields. By repeating this scheme, ground-state NH molecules can be accumulated in the magnetic trap. The crucial step in this approach is the transfer of stationary molecules into a trap in a dissipative fashion, and the underlying strategy is much more generally applicable than just to NH; similar schemes have been proposed

and used by others to accumulate atoms or molecules in magnetic or optical traps [7, 8].

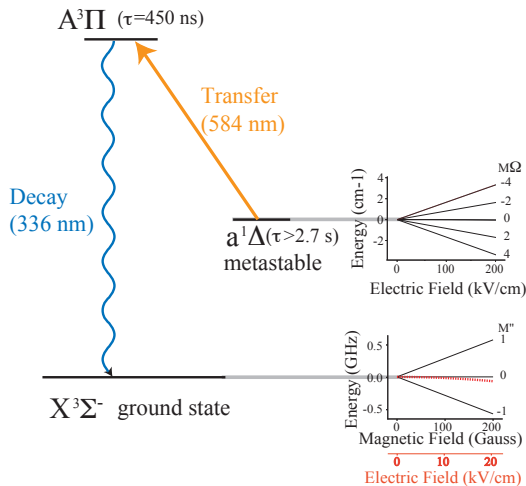


Fig. 1. Schematic representation of the electronic states of NH that are of relevance to the accumulation scheme. In the long-lived $a^1\Delta(v=0, J=2)$ state, the NH radicals experience a large Stark shift, as shown in the inset. Both the Stark shift (dashed curve) and the Zeeman shift (solid curves) of the lowest rotational level ($N''=0, J''=1$) in the $X^3\Sigma^-(v''=0)$ ground state as well. For the Stark shift, the different M -components are unresolved. Note the different scales for both insets (reprinted from [6]).

In Figure 1 the electronic states of the NH molecule that are of relevance to the accumulation scheme are schematically shown. The spin-forbidden $A^3\Pi(v'=0)\leftarrow a^1\Delta(v=0)$ transition around 584 nm, via which the NH molecules are optically pumped to the $X^3\Sigma^-(v''=0)$ ground state, has been observed and analyzed in detail before [9]. In that work, the (efficiency of the) various pathways to bring the metastable NH radicals to the lowest rotational level in the electronic and vibrational ground state has been discussed. We report here on the direct probing of the resulting population distribution of the rotational levels in the ground state of NH, using a pump-probe detection scheme. The production of an intense pulsed beam of metastable NH radicals, their deceleration to a standstill and their subsequent confinement in an electrostatic trap has also been previously reported upon [10]. Here, we report on the implementation of a quadrupole magnetic trap directly behind the Stark decelerator, following the approach demonstrated by others for ground-state OH radicals [11]. We first demonstrate magnetic trapping of the NH radicals in their metastable state. We then induce the unidirectional transfer of the metastable molecules to the ground state, and demonstrate magnetic trapping of ground-state NH molecules. By repeating the trap loading process, ground-state NH molecules from consecutive loading cycles are accumulated in the trap.

2 Experimental

For the formation of NH, a molecular beam of ≈ 1 vol % hydrazoic acid (HN_3) seeded in Kr is intersected with a focused 50 mJ/pulse beam of the fourth harmonic ($\lambda = 266$ nm) of a pulsed Nd:YAG laser (Quanta Ray, Indi Series) near the exit of a silica capillary mounted on the tip of a pulsed supersonic valve (Parker, General Valve). The HN_3 was prepared by the thermic reaction of sodium azide (NaN_3 , Sigma Aldrich) with an excess of lauric acid at $T=80^\circ\text{C}$ and $p=1$ mbar [12]. In this photodissociation scheme the majority of NH is formed in the desired $a^1\Delta$ state [13]. We used Kr as carrier gas even though its expansion forms a relatively fast beam ($v \approx 420\text{--}480$ m/s, Δv 20% FWHM) since the heavier Xe is known to efficiently quench the NH ($a^1\Delta$) molecules [13]. While the supersonic jet expansion assures an efficient rovibrational cooling of the nascent NH molecules in the $a^1\Delta$ electronic state, no electronic relaxation occurs. After passing a skimmer, a hexapole is used to couple the metastable NH radicals that are in low-field-seeking levels into the Stark decelerator. The molecular beam machine that has been used for these experiments [14] and its application to the deceleration of metastable NH radicals [10] have been described in detail before. For the experiment reported here, the decelerator serves the purpose to produce a spatially well-defined and slow packet of NH radicals in the $a^1\Delta(v=0, J=2)$ level.

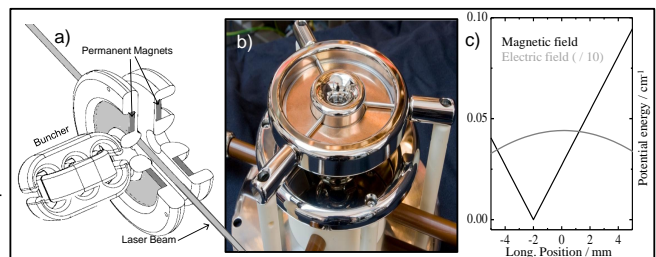


Fig. 2. Schematic drawing (a) and photograph (b) of the permanent magnetic trap. In (c) the loading potential and the trapping potential for NH ($a^1\Delta(v=0, J=2)$) radicals is shown with respect to the midpoint between the two disc-shaped electrodes.

After deceleration to a speed of about 20 m/s the molecular packet enters the magnetic trap. The trap consists of two disc-shaped nonmagnetic stainless steel electrodes placed 10 mm apart. Inside these electrodes strong permanent magnets are embedded, forming a quadrupole magnetic trap. Some of the technical details as well as a photograph of the trap can be seen in Figure 2. When the molecules enter this trap through a center hole in the first electrode, voltages of ± 20 kV are applied to the two electrodes. The slow molecules in their low-field-seeking state are stopped by the resulting electric field configuration that peaks in the center between the electrodes; there, the potential energy (Stark energy) of metastable NH radicals in the $J=2, M_J\Omega = -4$ level amounts to ≈ 0.35 cm^{-1} . The two permanent NdFeB N50 magnetic discs (IBS Mag-

net, Berlin) are aligned parallel to the electrodes and create a zero of the magnetic field at a position that is 2 mm closer to the exit of the decelerator than where the maximum of the electric field is. The depth of the magnetic trap is limited by the presence of the electrodes to 0.035 cm^{-1} (5.0 mK) and 0.053 cm^{-1} (7.6 mK) for metastable NH molecules in the ($J = 2, M = 2$) level and for ground-state NH molecules in the ($N'' = 0, J'' = 1, M'' = 1$) level, respectively. The laser light for the optical pumping and detection of the molecules passes through the center of the magnetic trap, perpendicular to the molecular beam axis. The laser induced fluorescence (LIF) is collected by a fused silica lens through a central hole in the last trapping electrode, spectrally filtered and detected by a photomultiplier tube.

The NH ($a^1\Delta$) radicals are detected by observing the $A^3\Pi \rightarrow X^3\Sigma^-$ fluorescence after driving the spin-forbidden $A^3\Pi \leftarrow a^1\Delta$ transition with the $\approx 50 \text{ mJ}$ output of a pulsed dye amplifier (Sirah, pumped by a Powerlite, Continuum), seeded at $\lambda = 584 \text{ nm}$ by a SHG Nd:YVO₄ (Millenia V, Spectra-Physics) pumped ring-dye laser (380A, Spectra-Physics). To probe the NH molecules in their $X^3\Sigma^-$ ground state, $\approx 3 \text{ mJ}$ of the $\lambda = 305 \text{ nm}$ output of a Nd:YAG (Surelight, Continuum) pumped pulsed dye laser (Narrowscan, Radiant-dyes) is used to excite the $A^3\Pi, v' = 1 \leftarrow X^3\Sigma^-, v'' = 0$ transition. As the electronic relaxation occurs predominantly via the diagonal $v' = 1 \rightarrow v'' = 1$ band, the fluorescence at $\lambda = 336 \text{ nm}$ can be readily separated from the scattered light of the excitation laser.

3 Results

3.1 Magnetic trapping of NH ($a^1\Delta$)

To optimize the relevant timings of the deceleration process, such as to produce a cloud of NH radicals with the highest possible density and the lowest possible temperature at the center of the magnetic trap, it is rather convenient that these radicals can also be magnetically trapped while in the metastable state. For optimum loading of the trap, the molecules need to have just the right amount of kinetic energy to overcome the potential barrier near the entrance of the magnetic trap and to subsequently be stopped by the electric field near the trap center. The density of magnetically trapped NH ($a^1\Delta, v = 0, J = 2, M = 2$) radicals was maximized by iteratively changing the experimental conditions while monitoring the intensity of the LIF at 336 nm. For this procedure, a set of parameters obtained from a one-dimensional trajectory calculation served as an initial guess. During the manual optimization, not surprisingly, the timings of the last few stages of the decelerator ("buncher" in Figure 2a) and of the loading potential proved to be most critical.

The measured intensity of the LIF signal at optimum settings is depicted in Figure 3 as a function of time after production of the metastable NH molecules via photolysis. The first maximum after around 8 ms results from the molecules that come to a standstill on the electrostatic stopping slope. The decelerated NH molecules are in the

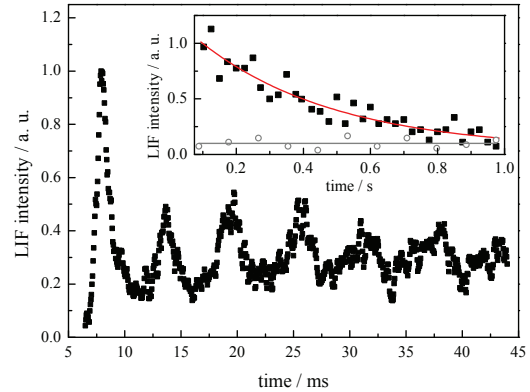


Fig. 3. Intensity of the LIF signal of NH ($a^1\Delta, v = 0, J = 2$) radicals at the center of the magnetic trap as a function of time. The slow metastable molecules enter the magnetic trap about 8 ms after their production in the beam source. Only half of the injected molecules will be in a magnetically low-field-seeking level and remain in the trap. Oscillations of the density of trapped metastable NH radicals at the trap center are clearly observed. In the inset, the intensity of the LIF signal is shown on a longer time-scale, both with (solid black squares) and without (open circles) metastable NH molecules in the trap, from which a $1/e$ trapping time of $350 \pm 40 \text{ ms}$ is deduced.

$M_J\Omega = -4$ component of the $J=2$ level (the M_J quantum number refers to the projection along the electric field), which splits into a $M = 2$ and a $M = -2$ component (M now refers to the projection along the magnetic field) in the magnetic field. Only the $M = 2$ component is low-field seeking in a magnetic field, thus explaining the reduction in fluorescence intensity after the first peak. As the trapping volume is large compared to the volume of the incoming packet of molecules and compared to the interaction volume with the laser, oscillations are observed in the fluorescence intensity. These oscillations, with a period of about 6 ms, reflect a 'breathing' like motion of the molecular ensemble in the trap. In the inset, the LIF signal is shown on a timescale of 1 second. The density in the trap is seen to exponentially decay with time, and a $1/e$ decay time of $350 \pm 40 \text{ ms}$ is extracted from these data. The dominant trap-loss channel is collisions with background gas in the approximately $3 \cdot 10^{-8} \text{ mbar}$ vacuum.

3.2 Optical pumping to the ground state

The uni-directional spontaneous decay from the $A^3\Pi$ state to the ground state is an essential step for the accumulation of ground-state NH molecules in a magnetic trap. The distribution over the ground-state ro-vibrational levels that occurs after spontaneous emission is governed by the Franck-Condon and Hönl-London factors. The $A - X$ transition in NH is almost perfectly diagonal and the $v' = 0 - v'' = 0$ band has a Franck-Condon factor of better than 0.999 [15]. To optimize the build-up of density in a single rotational level, preferentially the rotational ground state,

only the intermediate rotational level in the $A^3\Pi, v' = 0$ state needs to be chosen appropriately.

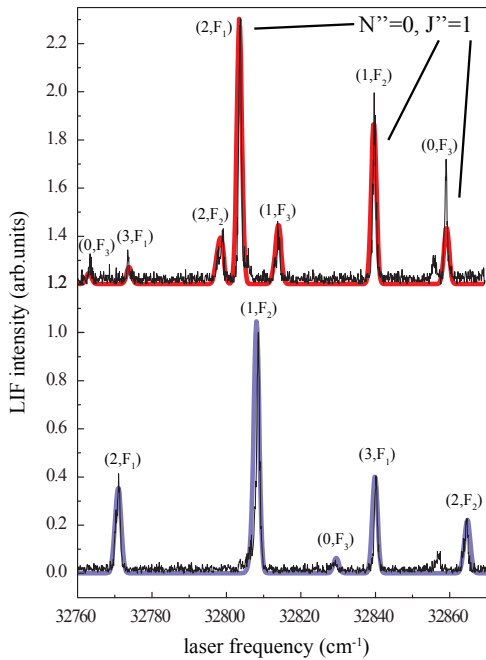


Fig. 4. Observed fluorescence excitation spectra, probing the population in the ground state of NH on the $A^3\Pi, v' = 1 \leftarrow X^3\Sigma^-, v'' = 0$ transition, together with simulated spectra. The upper and the lower spectrum, vertically offset for clarity, have been obtained after optical pumping from the metastable state via the positive and negative parity component, respectively, of the $J' = 1$ rotational level in the $A^3\Pi_1, v' = 0$ spin-orbit multiplet. The lines in the upper spectrum originate from the $N'' = 0, J'' = 1$ level when indicated and from the $N'' = 2$ level otherwise; all lines in the lower spectrum originate from the $N'' = 1$ level. The (J', F_i) labeling of the rotational levels in the $A^3\Pi$ state is given in the spectra.

In Figure 4, two different fluorescence excitation spectra, probing the population in the lowest rotational levels of the electronic and vibrational ground state, are shown. As the Λ -doublet splitting of the $a^1\Delta, v = 0, J = 2$ level is sub-MHz [16], both parity components of this metastable level are expected to be populated under our experimental conditions. The upper (lower) spectrum is obtained after optical pumping from the metastable state via the upper (lower) Λ -doublet component of the $J' = 1$ level in the $A^3\Pi_1$ spin-orbit manifold, via which exclusively ground-state levels with negative (positive) parity can be reached. The parity of the rotational levels in the $X^3\Sigma^-$ state is given by $(-1)^{N''+1}$, e.g. the $N'' = 0, J'' = 1$ ground-state level can only be reached via the upper Λ -doublet component of the $A^3\Pi_1, J' = 1$ level. Simulated spectra, using the known Hönl-London factors for the spontaneous decay from the selected rotational levels in the $A^3\Pi, v' = 0$ state as well as for the excitation from the ground state to the $A^3\Pi, v' = 1$ state, are shown as solid curves in both spectra and are seen to reproduce the observations very well.

The three strongest lines in the upper spectrum all originate from the lowest rotational level in the $X^3\Sigma^-, v'' = 0$ ground state of NH, as explicitly indicated in the Figure; the four remaining fitted lines originate from the different spin components of the $N'' = 2$ level. The $R_{P_{31}}(1)$ transition around 32860 cm^{-1} is observed to be stronger than expected from the simulations; although care was taken not to saturate the transitions, this has probably not been completely avoided in the measurements. All fitted lines in the lower spectrum originate from the different spin components of the $N'' = 1$ level. To identify the transitions, the (J', F_i) labeling of the rotational levels in the $A^3\Pi$ state (F_1 for $^3\Pi_2$; F_2 for $^3\Pi_1$; F_3 for $^3\Pi_0$) is given in the spectra [17]. The small peaks in the measured spectra around 32807 and 32857 cm^{-1} originate from rotational transitions in the $c^1\Pi, v' = 1 \leftarrow a^1\Delta, v = 0$ band that happen to lie in the same spectral region.

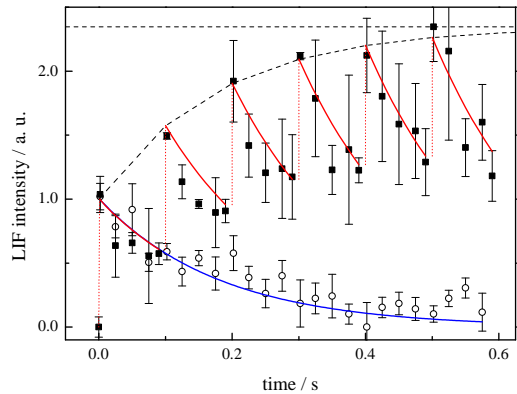


Fig. 5. Intensity of the LIF signal of trapped ground-state NH molecules as a function of time. At time equal zero the ground-state molecules are produced. The measured LIF signal is shown after a single loading event (open circles) and over the course of six consecutive loading cycles (solid squares), together with the best fitting curves, shown in blue and red, respectively. The intensity of the LIF signal immediately after a loading event converges to the value indicated by the dashed horizontal line.

3.3 Accumulation of ground-state NH molecules

The slow ground-state NH molecules are created near the center of the quadrupole magnetic trap and can remain trapped, provided they have a sufficiently low kinetic energy. To detect these trapped molecules, the same off-resonant LIF detection scheme as described in the previous paragraph is used. By recording the LIF signal as a function of time after production of the ground-state molecules, the time-dependence of the density in the trap can be monitored. In Figure 5 the LIF signal of trapped NH ($X^3\Sigma^-, v'' = 0, N'' = 0, J'' = 1, M'' = 1$) molecules is shown after loading a single packet into the magnetic trap

(open circles). It is difficult to extract the density of trapped molecules from a measurement of this type, but we estimate to have about 10^4 ground-state NH molecules in the trap, at a density of about $10^5/\text{cm}^3$. From a fit of these data to an exponentially decaying curve, a $1/e$ trapping time of $\tau = 180 \pm 20$ ms is deduced. This trapping time is shorter than observed for the metastable NH molecules, probably because the background pressure was slightly higher during the accumulation measurements.

As the pulsed molecular beam machine and the laser systems are running at a repetition frequency f of 10 Hz, every 0.1 s a new packet of Stark-decelerated NH molecules arrives near the trap center and can be transferred to the ground state. Although the pulsed beam of carrier gas and undecelerated NH radicals also passes through the trap, its density is rather low there and is not expected to lead to any observable trap loss. The intensity of the LIF signal that is observed when six consecutive packets of NH molecules are accumulated in the magnetic trap is shown in Figure 5 as well (solid black squares). At any time during the trapping process, the LIF signal is expected to show an exponential decay with the same time constant τ mentioned above. Under the assumption that the density of molecules that is added to the trap per deceleration cycle is always the same, the LIF signal immediately after loading the n -th ($n \geq 1$) packet is a factor

$$\sum_{i=0}^{n-1} e^{-i/f\tau} \quad (1)$$

larger than the signal immediately after loading the first packet. A fit of the data according to this model, in which the overall vertical scale is the only adjustable parameter, is shown as well. The sum in the equation above converges to a value of $1/(1 - e^{-1/f\tau})$, which is indicated by the horizontal dashed line in Figure 5. In the present experiment, we can at most increase the density of accumulated molecules by a factor 2.35 (± 0.20) relative to the density after a single loading event. This limiting value is already almost reached after loading six packets, which is why we limited the loading sequence to this.

4 Conclusions

The results presented here demonstrate that the scheme proposed about a decade ago to accumulate ground-state NH radicals in a magnetic trap indeed works [6]. At the same time, it shows the limitations of this approach, as the gain in density that has been obtained thus far has only been slightly more than a factor of two. One might wonder whether an equally large gain could have been obtained by using a single loading cycle and by having the molecular beam source further optimized instead, for instance, and this might indeed well have been the case. If one would like to pursue accumulation of multiple packets in the trap in the future, one has to make the product $f\tau$ (which is the convergence limit of the sum in equation (1) when $f\tau \gg 1$) as large as possible, i.e. one has to increase

the product of the repetition frequency with which the trap can be reloaded and the trapping time. Given that in the present experiment the NH molecules are transferred into the magnetic trap within 10 milliseconds after they leave the beam source, the repetition frequency could in principle be an order of magnitude larger. To increase the trapping time, the rate of collisions with background gas has to be reduced, i.e. the vacuum needs to be improved. Losses due to nonadiabatic transitions near the trap center have to be avoided as well, and a Ioffe-Pritchard type magnetic trap might be required. At some point, losses due to optical pumping by blackbody radiation will become the dominating loss channel [18], in which case one would need to cool the trap. It has recently been demonstrated that in a cryogenic setup, ground-state NH molecules can be magnetically trapped with $1/e$ lifetimes of over 20 seconds [19]. In such a cryogenic trap, the density could be increased by more than a factor of 200 via this accumulation scheme, even with reloading at the present frequency of 10 Hz.

5 Acknowledgements

This work is supported by the ESF EuroQUAM programme, and is part of the CoPoMol (Collisions of Cold Polar Molecules) project. We thank Henrik Haak for the design of the integrated magnetic trap and Boris G. Sartakov for his help with the analysis of the observed LIF spectra. WJ thanks the Alexander von Humboldt Foundation for a Research Award.

References

1. *Cold Molecules: Theory, Experiment, Applications*, edited by R.V. Krems, W.C. Stwalley and B. Friedrich (Taylor & Francis Group, Boca Raton, FL, 2009).
2. L.D. Carr, D. DeMille, R.V. Krems and J. Ye, *New J. of Phys.* **11**, (2009) 055049.
3. J.D. Weinstein, R. deCarvalho, T. Guillet, B. Friedrich and J.M. Doyle, *Nature* **395**, (1998) 148.
4. S.Y.T. van de Meerakker, H.L. Bethlem and G. Meijer, *Nature Physics*, **4**, (2008) 595, and references therein.
5. E.S. Shuman, J.F. Barry and D. DeMille *Nature* **467**, (2010) 820.
6. S.Y.T. van de Meerakker, R.T. Jongma, H.L. Bethlem and G. Meijer, *Phys. Rev. A* **64**, (2001) 041401.
7. J. Stuhler, P.O. Schmidt, S. Hensler, J. Werner, J. Mlynek and T. Pfau, *Phys. Rev. A* **64**, (2001) 031405.
8. E. Narevicius, S.T. Bannerman and M.G. Raizen, *New J. of Phys.* **11**, (2009) 055046.
9. S.Y.T. van de Meerakker, B.G. Sartakov, A.P. Mosk, R.T. Jongma and G. Meijer, *Phys. Rev. A* **68**, (2003) 032508.
10. S. Hoekstra, M. Metsälä, P.C. Zieger, L. Scharfenberg, J.J. Gilijamse, G. Meijer and S.Y.T. van de Meerakker, *Phys. Rev. A* **76**, (2007) 063408.
11. B.C. Sawyer, B.K. Stuhl, D. Wang, M. Yeo and J. Ye, *Phys. Rev. Lett.* **101**, (2008) 203203.
12. J.R. McDonnald, J.W. Rabalais and S.P. McGlynn, *J. Chem. Phys.* **52**, (1970) 1332.

13. S.Y.T. van de Meerakker, I. Labazan, S. Hoekstra, J. Küpper and G. Meijer, *J. Phys. B.* **39**, (2006) 1077.
14. S.Y.T. van de Meerakker, N. Vanhaecke and G. Meijer, *Ann. Rev. Phys. Chem.* **57**, (2006) 159.
15. D.R. Yarkony, *J. Chem. Phys.* **91**, (1989) 4745.
16. W. Ubachs, G. Meyer, J.J. ter Meulen and A. Dymanus, *J. Mol. Spectr.* **115**, (1986) 88.
17. R.N. Dixon, *Can. J. Phys.* **37**, (1959) 1171.
18. S. Hoekstra, J.J. Gilijamse, B. Sartakov, N. Vanhaecke, L. Scharfenberg, S.Y.T. van de Meerakker and G. Meijer, *Phys. Rev. Lett.* **98**, (2007) 133001.
19. E. Tsikata, W.C. Campbell, M.T. Hummon, H-I. Lu and J.M. Doyle, *New J. Phys.* **12**, (2010) 065028.